Nonperturbative terahertz-field interactions in semiconductor quantum wires

S. Hughes
Department of Physics, University of Surrey, Guildford, Surrey GU2 7XH, United Kingdom
(Received 26 July 2000; published 28 March 2001)

We model high-field dynamic electro-optical effects in semiconductor quantum wires. Our nonperturbative, time-dependent studies employ weak optical pulses and strong terahertz fields such as are available from free-electron lasers. Three remarkably strong effects are demonstrated: (1) a strong Autler-Townes splitting of the 1*s* exciton resonance via intraband exciton coupling, (2) phase-dependent two-photon induced gain just above the band gap, and (3) high-field harmonic generation in the THz regime.

DOI: 10.1103/PhysRevB.63.153308 PACS number(s): 42.50.Md, 42.65.Ky, 71.35.−y, 78.47.+p

Electroabsorption is the phenomenon of absorption changes in a material in response to an electric field. In bulk semiconductors the Franz-Keldysh[1] effect takes place when a strong dc field **F** is applied. With the advent of quantum wells, electroabsorption studies have continued to receive intense interest because quantum confinement systems show especially strong electroabsorption effects, for example, the quantum-confined Stark effect.[2] Surprisingly, for quantum-well wires (QWW's) no such investigations were undertaken until very recently.[3] However, QWW's are in fact probably the most intruiging system to study since they offer very close analogies with the high-field physics of atomic ensembles; they also achieve the most dramatic effects such as self-induced transparency.[3] A possible theoretical deterrent for high-field predictions in QWW's is the well known inverse-square-root divergence of the joint density of states at the band gap. However, the intensity ratio of the optical density associated with excitonic scattering states to the free electron-hole (e-h) pair above the band gap— the Sommerfeld factor—removes this divergence.[4] Consequently, the QWW system remains entirely physical as long as one treats excitons exactly. Although high-field atomic physicists have been exploring Coulomb ionization effects intensely for one-dimensional (1D) atomic systems,[5] little is known about the electro-optical properties of related semiconductor environments. Both experimental[6] and theoretical[7,8] studies of QWW's are being carried out for device applications such as semiconductor lasers.[9] Moreover, excellent strides in growth technologies for semiconductor nanostructures have resulted in renewed interest in QWW's, resulting in the development of high-quality samples with well defined characteristics.

Recently, a relatively new area of high-field physics has emerged, namely, the dynamic response of semiconductors to intense time-dependent electric fields $\mathbf{F}(t)$. For example, for terahertz-frequency driving fields Ω, the dynamic Franz-Keldysh effect has been theoretically predicted[10] and experimentally verified[11] using free-electron lasers (FEL's). Terahertz emitters are a welcome tool for exploring the dynamics of semiconductor nanostructures since they offer a combination of optics and high-speed transport. With regard to superlattices, various effects including Zenner tunneling,[12] collapse of the miniband,[13] dynamic localization,[14] and reflection of THz radiation[15] have emerged. As well as having a wide range of applications, high-field dynamical effects in 1D semiconductors are also of fundamental interest. Indeed, the collective theme of our investigation, namely, the response of matter to high fields where perturbation theory in the field strengths provides an inadequate description, has a potentially vast audience

In the domain of high-field atomic physics a related study of interest is high-harmonic generation (HHG). The process of HHG due to an intense atom-field interaction has received a great deal of attention in recent years,[16–18] and coherent short-wavelength radiation well into the x-ray region has been demonstrated. Moreover, harmonically generated x-ray transients as short as 100 as have been predicted.[19] The observed spectrum of harmonics is affected by both the single-atom emission and the ensuing collective behavior. We are interested in exploring related phenomena involving harmonic generation for the QWW but in the THz regime. The theoretical treatment of HHG is most fruitfully described in terms of quantum wave packets (WP's). Semiconductor physicists, however, rarely think of WP's, and theoretical studies are typically carried out in energy (k) space because of translational invariance. On the contrary, we will show in this work that the dynamics of QWW's excited hybridly by a subpicosecond laser and a strong polarized THz field is ideally studied in terms of WP's.

For a simple interband excitation, the THz field can be accounted for nonperturbatively by employing an effective 1D Schödinger equation (in excitonic units)

$$i\frac{\partial}{\partial t}\Psi(x,t)=\left[E_{\mathrm{g}}-\frac{\partial^2}{\partial x^2}-V(x)+x\mathbf{F}(t)\right]\Psi(x,t), \qquad (1)$$

where x is the relative distance between an electron and hole, $\Psi(x,t)$ is the quasi-one-dimensional WP, $\mathbf{F}(t)=\hat{\mathbf{n}}_x F_0 \sin(\Omega t+\phi)$ is the THz electric field polarized along the wire axis with frequency Ω and phase ϕ (at the center of the optical pulse $t=0$), $\hat{\mathbf{n}}_x$ a unit vector in the QWW axis, and V is the Coulomb potential whose specific form is discussed below. F_0, the magnitude of the THz field, is taken to be 8 kV/cm with a corresponding field energy $E=eF_0a_0=3E_0$, where a_0 and E_0 are the the 1s Bohr radius and binding energy, respectively. The approach has two key attractions: first it allows us to probe quantum mechanically the relative e-h WP motion, and secondly we can exploit a very efficient fast Fourier transform algorithm developed already for high-field studies of atomic media. The quantum method for integrating Eq. (1) numerically *without using a*

restrictive basis expansion can be implimented by employing the split-step method.[20,21] The core of this method is to carry out the action of the kinetic operator efficiently in Fourier space, while the action of the potential operator is carried out in real space. Unlike the atomic studies, we are interested in the optical properties and thus need to consider the original source, i.e., an optical field, and hence we reformulate the WP equation in terms of the polarization. Assuming only the $1e$ subband (a) and various h subbands (b) (see below for more details),

$$i\frac{\partial}{\partial t}P_{ab}(x,t)=\left[E_{\mathrm{g}}-\frac{\partial^2}{\partial x^2}+x\mathbf{F}(t)-i\Gamma\right]P_{ab}(x,t)$$

$$-\sum_{\beta}V_{ab}^{a\beta}(x)P_{a\beta}(x,t)+\Omega_{ab}(t)\,\delta(x), \quad (2)$$

where $\Omega_{ab}(t)=d_{ab}\varepsilon(t)$ is the Rabi energy with d_{ab} the interband dipole moment and $\varepsilon(t)$ the optical pulse, Γ^{-1} is the dephasing time, and P_{ab} is the induced polarization between two subbands a (electrons) and b (holes); we note that the total polarization is in general an infinite summation over all subbands, although accurate simplifications can be made. We choose an optical pulse that is excited resonantly with the band gap.

For a tractable model for the QWW potential we will assume that the electrons and holes are confined laterally by a harmonic oscillator potential with a subband spacing of $\Omega_{j=e,h}$. Moreover, we assume perfect confinement in the growth direction (i.e., only one associated subband). The Coulomb interaction between charge carriers thus becomes (in excitonic units) $V_{ab}^{a\beta}(x)=2\int dy\int dy'\,\psi_a(y)\psi_b^*(y')\psi_a(y)\psi_\beta^*(y')/\sqrt{x^2+(y-y')^2}$, where $\psi_j(y)$ are the eigenfunctions[8] associated with the lateral carrier motion,

$$\psi_n^{j=e,h}(y)=\left(\frac{1}{2^n n!}\sqrt{\frac{\mu\Omega_j}{m_j 2\pi}}\right)^{1/2}$$

$$\times\exp[-(\mu\Omega_j/m_j)y^2]H_n\left(\sqrt{\frac{\mu\Omega_j}{2m_j}}y\right),$$

with μ the reduced mass, m_j the mass of an electron or hole, and H_n the Hermite polynomial. The Fourier transform of Eq. (2) is exactly equivalent to the semiconductor Bloch equations in the low-density limit.[22,23] The real-space approach has been exploited already to obtain the static Franz-Keldysh effect in QWW's.[3].

To begin we employ a multisubband model with one conduction subband ($1e$) and four valence subbands (1hh,2hh,3hh,4hh). Since we are dealing with symmetric wires for this study only two WP's contribute to the optical properties at low density: P_{11} and P_{13}. Consequently we now have to solve two polarization equations that are coupled through the Coulomb matrix elements. Full Coulombic coupling is taken into account self-consistently by calculating the appropriate Coulomb and interband matrix elements. We mention, however, that essentially all the important dynamics can be obtained by assuming a two-subband semiconductor model ($ab=1e-1\mathrm{hh}$) since P_{11} is by far the predominant WP for this particular study; the additional subbands are included for completeness. The interplay between the THz field and the excitonic Coulomb interactions is included to all orders.

We take material parameters typical of GaAs with a bulk exciton binding energy $E_0=4.2$ meV, Bohr radius $a_0=140$ Å, and interband dipole moment $d=3\ e$ Å (d_{ab} is subsequently obtained by integrating over the appropriate eigenfunctions). For the eigenfunction calculations we choose subband spacings of $3E_0$ for the holes and $7E_0$ for the electrons, and $m_h=5m_e$. This results in holes that are more strongly confined than the electrons. For the purpose of obtaining a relevant observable we assume an array (1D sheet) of thin QWW's where the transmitted pulse can be obtained exactly from $\varepsilon_t(t)=\varepsilon_0(t)+iKP_{\mathrm{opt}}(t)$ with K a constant; the polarization and electric field are slowly varying quantities. The optical polarization is simply $P_{\mathrm{opt}}(t)=\Sigma_\beta d_a P_{a/\beta}(x=0,t)$. For the electric field a *weak* Gaussian pulse with a 40 fs full width e^{-2} maximum irradiance is chosen. We choose a real-space region of $\pm 150a_0$ with 4096 discretized spatial points, and numerically propagate with a time step of 0.1 fs. The computational technique is extremely efficient, requiring only several minutes CPU time per run (typically for a 10 ps simulation).

We first calculate absorption properties with a dephasing time of 500 fs in the absence of an external field $\mathbf{F}(t)$. Figure 1(a) shows the input pulse (dashed curve), transmitted pulse (solid curve), and their ratio (dotted curve), which gives a measure of the spectral absorption. (We note that a proper cw absorption spectrum cannot be obtained here since we are dealing with time-dependent THz fields and optical pulses; thus as we shall see even the phase will play a crucial role on the ensuing dynamics.) As expected the Coulomb interaction removes the singularity at the band gap associated with the 1D density of states.[4,22] The $1s$ binding energy is about 11 meV and the absorption spectrum exhibits two peaks separated by $6E_0$ (twice the subband spacing). Next we add an electric field aligned along the QWW axis (x direction). In Figs. 1(b), 1(c), and 1(d) we show the input and transmitted irradiances for $\Omega=2$ THz, 2.5 THz, and 3 THz, respectively; the phase $\phi=0$. In Fig. 1(b) not only do we see spectral gain (which is discussed in more detail below) but, in addition to a reduction of the $1s$ oscillator strength, there is a clear absorption splitting of the fundamental exciton resonance. A single THz photon resonance from this splitting lies just below the band edge, i.e., the splitting energy plus a THz photon energy lies just below the gap. Therefore what we are obtaining here is analagous to the well known Autler-Townes splitting for three-level atoms. The physics behind this phenomenon is to introduce a third level to a two-level system whereby the third level coherently couples to one of the other levels. Thus when two appropriately tuned fields are applied the usual absorption spectrum has a large dip in its absorption resonance due to the coherent coupling to the third level. In the present case, however, the third level coherence is achieved via intraband coupling of the lowest ($1s$) and higher exciton states lying just below the band edge. In essence the higher-lying exciton states are now co-

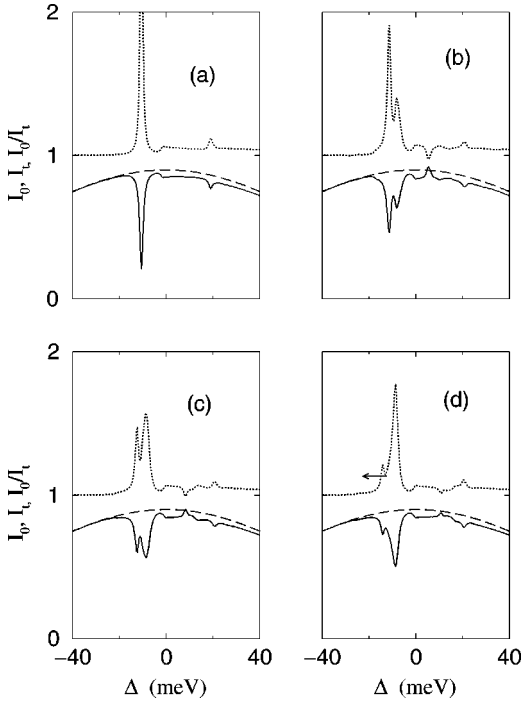

FIG. 1. (a) In the absence of $\mathbf{F}(t)$. Input pulse (dashed curve), transmitted pulse (solid curve), and their ratio (dotted curve), which gives a measure of the absorption. (b) As in (a) with $\mathbf{F}(t)$ ($F_0=8$ kV/cm) applied and $\Omega=2$ THz. (c) As in (a) with $\mathbf{F}(t)$ applied and $\Omega=2.5$ THz. (d) As in (a) with $\mathbf{F}(t)$ applied and $\Omega=3$ THz; the arrow shows the redshift of the local minimum (see text).

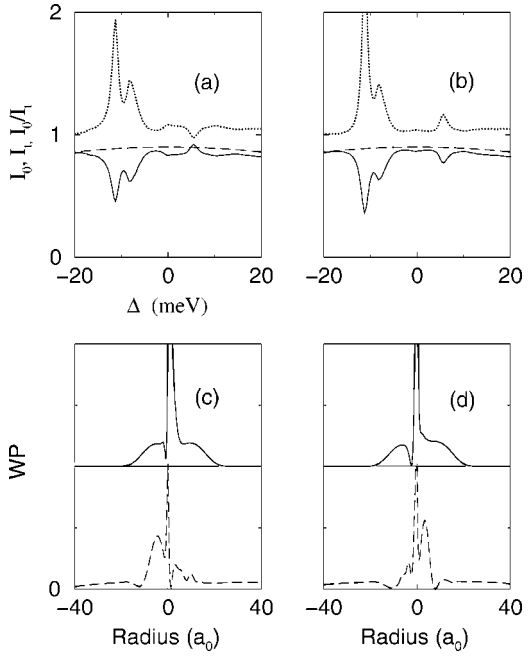

FIG. 2. (a) Input pulse (dashed curve), transmitted pulse (solid curve), and their ratio (dotted curve), which gives a measure of the absorption. The THz frequency is $\Omega=2$ THz with $\phi=0$. (b) As in (a) with $\phi=\pi/2$. (c) WP (P_{11}) at several times (solid curve, $t=200$ fs, and dashed curve, $t=600$ fs) corresponding to (a). A displacement of the WP from $x=0$ means it is polarized. (d) WP (P_{11}) at several times (solid curve, $t=200$ fs, and dashed curve, $t=600$ fs) corresponding to (b).

herently coupled to the lowest state by the THz field. This is the only possible explanation for such a splitting. To clarify this mechanism we can see that the region of induced transmission (local resonance minimum) gradually redshifts proportionally with an increasing THz photon energy and eventually disappears when the THz photon energy becomes greater than the $1s$ exciton binding energy; to highlight the redshift, for clarity, an arrow is shown in Fig. 1(d). This is expected as there is no dipole coupling between exciton and continuum states. The effect of the higher subband does not play any significant role for our chosen QWW.

Next we investigate the phenomenon of two-photon gain which results in a small gain peak in the absorption spectrum. These effects will be quite distinct from the above one-photon scenario as they will appear as large changes in the spectrum in the region 2Ω above the $1s$ resonance in the continuum. Figures 2(a) and 2(b), respectively, show the $\Omega=2$ THz simulations with a phase of $\phi=0$ and $\phi=\pi/2$. As can be recognized the two-photon replica can be induced gain or induced absorption depending on the initial phase of the WP's. The two-photon effects are very strong and can be easily tuned simply by changing the frequency of the THz driving field.

A displacement of the WP from $x=0$ means it is polarized. In Figs. 2(c) and 2(d) are shown snapshots of the polarization WP ($|P_{11}(x,t)|^2$) at times 200 fs (solid curve) and 600 fs (dashed curve). The time $t=200$ fs depicts the WP shortly after the optical pulse has gone, where there is a strong probability for the electrons and holes to be Coulombically bound. At later times the WP spreads and quantum beating occurs between the continuum states and the excitonic states. Spatial interference occurs from the combination of slow relative-coordinate space and the formation of sidelobes in the WP; these are formed by the combination of slow transverse spreading, the relatively fast field-driven motion in the polarization direction, and the excitonic attraction (Coulombic rescattering). In the context of excitonic attraction, Coulombic rescattering is associated with the reencounter of the photogenerated electrons and holes as the THz field not only pulls the e-h pairs apart, but also pushes them back together again. Wave packet spreading and phase lag associated with the reencounters lead to spatial interference.

The elegance of the WP approach is that it gives us simultaneous optical and THz information. We now turn our attention to the THz dynamics. The THz-induced intraband dipole moment $P_{\mathrm{THz}}(t)=e\int dx P^*(x,t)xP(x,t)$, and for the emitted THz electric field—assuming a point source—$E_{\mathrm{THz}}(t)\propto\ddot{P}_{\mathrm{THz}}(t)$. In Fig. 3 we show the emitted THz field versus t for the phases (at $t=0$, center of the optical pulse) of $\phi=0$ (a) and $\pi/2$ (b), for the 2 THz field. Each transient is approximately 3 ps in duration reflecting the combined effect of WP spreading and dephasing. We note that the time $t=0$ corresponds to the center of the optical pulse and hence has a finite contribution. In the corresponding electromagnetic spectra [Figs. 3(c) and 3(d)], a series of harmonics separated in frequency by approximately 2Ω appear in the THz regime. (Of course they are not exactly spaced by 2Ω

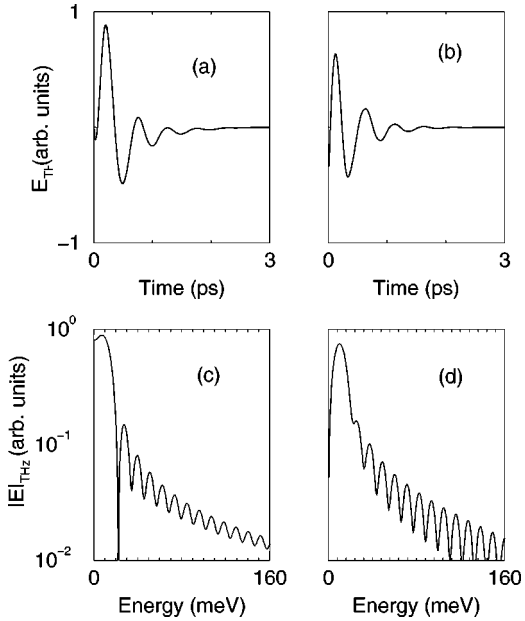

FIG. 3. (a) Emitted THz field as a function of time with $\phi=0$ and $\Omega=2$ THz. (b) As in (a) with $\phi=\pi/2$. (c) Corresponding spectrum to (a). (d) Corresponding spectrum to (b).

as here we are dealing with spectrally broad short pulses and nonperturbative effects.) Although these spectra do not seem to form any plateaus[17] (an extensive region of similar spectral intensity in frequency extending well above the fundamental excitonic binding energy), the amount of additional frequency components is quite substantial surpasses the harmonics achievable in quantum wells.[24] Furthermore, these sorts of measurement may form an appropriate technique for (1) measuring the phase of the original THz wave form, which is not an easy task for high fields and in particular for FEL's, and (2) emitting transients in the tens-of-THz regime. For Rydberg atoms,[25] higher-frequency harmonics are produced from continuum-state to bound-state transitions, in which electrons release the energy absorbed from the field during its excursion in the continuum. A similar mechanism is at work here when the ponderomotive energy of the *e-h* pair becomes comparable to or greater than the bound states' energy. (Our value of $F_0=8$ kV/cm was chosen to produce ponderomotive energies comparable to the 1*s* binding energy.)

In conclusion, we have studied the dynamics of the high-field THz Franz-Keldysh effect and exciton ionization in QQW's by solving the semiconductor Bloch equations in real space. Real-space and real-time effects were studied by probing the *e-h* wave packet motion. For a THz photon just below the 1*s* binding energy, a strong Autler-Townes splitting of the exciton was obtained. By using coherent control, two-photon induced gain (or absorption) can be achieved in the continuum. Finally, the emission of phase-dependent spectra in the THz regime was demonstrated, analogous to the high-field physics of atomic ensembles. A more detailed probe into the differences between one- and three-dimensional semiconductors is the subject of future work.

Stimulating discussions with Ben Murdin and David S. Citrin are gratefully acknowledged.

[1] W. Franz, Z. Naturforsch. 4 **13**, 484 (1958); Sov. Phys. JETP **34**, 788 (1958).
[2] S. Schmitt-Rink *et al.*, Adv. Phys. **38**, 89 (1989).
[3] S. Hughes and D. S. Citrin, Phys. Rev. Lett. **84**, 4228 (2000).
[4] T. Ogawa and T. Takagahara, Phys. Rev. B **44**, 8138 (1991).
[5] U. Schwengelbeck and F.H.M. Faisal, Phys. Rev. A **50**, 632 (1994).
[6] See, for example, R. Rinaldi *et al.*, Phys. Rev. Lett. **73**, 2899 (1994); C. Constantin *et al.*, Phys. Rev. B **59**, R7809 (1999); K.H. Wang *et al.*, *ibid.* **53**, R10 505 (1996); W.R. Tribe *et al.*, Appl. Phys. Lett. **73**, 3420 (1998).
[7] See, for example, F. Tassone and C. Piermarocchi, Phys. Rev. Lett. **82**, 843 (1999); F. Rossi *et al.*, *ibid.* **78**, 3527 (1997); S. Das Sarmal and E.H. Hwang, Phys. Rev. B **54**, 1936 (1996); O. Mauritz *et al.*, Phys. Rev. Lett. **82**, 847 (1999).
[8] D.B. Tran Thoai and H. Thien Cao, Solid State Commun. **111**, 67 (1999).
[9] See, for example, J. Wang *et al.*, Appl. Phys. Lett. **69**, 287 (1996); G. Lehr *et al.*, *ibid.* **68**, 2327 (1996); S. Tiwari and J.M. Woodall, *ibid.* **64**, 2211 (1994).
[10] A.P. Jauho and K. Johnsen, Phys. Rev. Lett. **24**, 4576 (1996).
[11] K.B. Nordstrom *et al.*, Phys. Status Solidi B **204**, 52-54 (1997).
[12] F. Bloch, Z. Phys. **52**, 555 (1929).
[13] M. Holthaus, Phys. Rev. Lett. **69**, 351 (1992).
[14] T. Meier *et al.*, Phys. Rev. Lett. **73**, 902 (1994).
[15] A.W. Ghosh, A.V. Kuznetsov, and J.W. Wilkins, Phys. Rev. Lett. **79**, 3494 (1997); J. Kono *et al.*, *ibid.* **79**, 1758 (1997).
[16] M. Protopapus, D.G. Lappas, and P.L. Knight, Phys. Rev. Lett. **79**, 4550 (1997); G.G. Paulus *et al.*, *ibid.* **80**, 484 (1998).
[17] P. Moreno, L. Plaja, and L. Roso, J. Opt. Soc. Am. B **13**, 430 (1996).
[18] J. Zhou *et al.*, Phys. Rev. Lett. **76**, 752 (1996).
[19] I.P. Christov, M.M. Murname, and H.C. Kapteyn, Phys. Rev. Lett. **78**, 1251 (1997).
[20] R. Grobe and J.H. Eberly, Phys. Rev. A **48**, 4664 (1993).
[21] M. Protopapas *et al.*, Phys. Rev. Lett. **23**, 4550 (1997).
[22] See, H. Haug and S.W. Koch, *Quantum Theory of the Optical and Electronic Properties of Semiconductors*, 3rd ed. (World Scientific, Singapore, 1994), and references therein.
[23] R. Zimmermann, in *Spectroscopy and Dynamics of Collective Excitations in Solids*, edited by X. Di Bartoli (Plenum Press, New York, 1997), p. 126.
[24] S. Hughes and D.S. Citrin, Phys. Rev. B **59**, R5288 (1999); D.S. Citrin and S. Hughes, *ibid.* **60**, 13 272 (1999).
[25] J.L. Krause *et al.*, Phys. Rev. Lett. **79**, 4978 (1998).